ORIGINAL ARTICLE

European Archives of Medical Research

DOI: 10.14744/eamr.2026.04900

Eur Arch Med Res 2026;42(3):302-309

Magnetic Resonance Imaging Evaluation of Neural Injury Spectrum and Associated Secondary Musculoskeletal Sequelae in Obstetric Brachial Plexus Palsy

Seda Kaynak Sahap,[1] Eda Almus,[1] Berna Ucan,[2] Suat Fitoz[1]

[1]Department of Pediatric Radiology, Ankara University, Faculty of Medicine, Ankara, Türkiye

[2]Department of Pediatric Radiology, Ankara Etlik City Hospital, Ankara, Türkiye

ABSTRACT

Objective: The aim of this study was to characterize the spectrum of neural injury patterns and secondary musculoskeletal abnormalities on magnetic resonance imaging (MRI) in children with obstetric brachial plexus palsy (OBPP).

Materials and Methods: In this retrospective descriptive study, 56 children with OBPP who underwent brachial plexus MRI were included in the study. MRI examinations were reviewed for preganglionic and postganglionic abnormalities, distal plexus involvement, denervation-related muscle changes, and posterior humeral head subluxation. Patients were categorized as having pure preganglionic, pure postganglionic, or mixed injury patterns. Associations between muscle abnormalities, posterior humeral head subluxation, injury patterns, and patient age were evaluated using Chi-square, Fisher's exact, and Mann–Whitney U-tests, as appropriate.

Results: The median age at MRI was 10.8 months. Pure preganglionic injury was identified in 15 patients (26.8%), pure postganglionic injury in 24 (42.9%), and mixed injury in 17 (30.4%). Overall, root involvement was most frequent at C6 (83.9%), followed by C7 (75.0%) and C5 (60.7%). Neuroma-like nodular thickening was observed in 16 patients (28.6%). Muscle atrophy was present in 44 patients (78.6%), muscle edema in 13 (23.2%), and posterior humeral head subluxation in 44 patients (78.6%). An association was observed between subscapularis muscle atrophy and posterior humeral head subluxation (84.1% vs. 50.0%, $p=0.022$). Patients with muscle edema were significantly younger than those without edema ($p<0.001$).

Conclusion: OBPP demonstrates a broad spectrum of neural and musculoskeletal abnormalities on MRI. In addition to characterizing preganglionic and postganglionic injury patterns, MRI provides valuable information regarding denervation-related muscle changes and secondary shoulder deformity, enabling comprehensive assessment of disease involvement.

Keywords: Brachial plexus injuries, magnetic resonance imaging, muscle atrophy, obstetric brachial plexus palsy, shoulder subluxation

Cite this article as: Kaynak Sahap S, Almus E, Ucan B, Fitoz S. Magnetic Resonance Imaging Evaluation of Neural Injury Spectrum and Associated Secondary Musculoskeletal Sequelae in Obstetric Brachial Plexus Palsy. Eur Arch Med Res 2026;42(3):302-309.

Address for correspondence: Seda Kaynak Sahap. Department of Pediatric Radiology, Ankara University, Faculty of Medicine, Ankara, Türkiye

E-mail: dr.seda@gmail.com **ORCID ID:** 0000-0003-1283-9543

Submitted: 18.06.2026 **Revised:** 07.07.2026 **Accepted:** 08.07.2026 **Available Online:** 18.09.2026

European Archives of Medical Research – Available online at www.eurarchmedres.org

INTRODUCTION

Obstetric brachial plexus palsy (OBPP) is one of the most common peripheral nerve injuries in newborns and results from traction injury to the brachial plexus during delivery. The severity of injury ranges from transient neuropraxia to complete root avulsion and may result in persistent motor deficits, muscle imbalance, glenohumeral deformity, and long-term functional impairment.[1,2]

Although many infants with OBPP experience spontaneous functional recovery, a subset develop persistent neurological deficits that may require imaging evaluation and surgical consideration.[2,3] Accurate characterization of the location and extent of neural injury is therefore essential for treatment planning and prognostic assessment. Clinical examination and electrodiagnostic studies provide important information regarding functional impairment; however, they may be limited in young infants and may not accurately localize the level of injury.[4] Although surgical exploration remains the reference standard for defining the extent of neural injury, its invasive nature limits its use as a diagnostic tool.[2,3] Magnetic resonance imaging (MRI) has emerged as a valuable non-invasive modality for evaluating both preganglionic and postganglionic components of the brachial plexus.[4,5] In addition to identifying root avulsion and pseudomeningocele formation, MRI provides comprehensive assessment of postganglionic nerve abnormalities and denervation-related musculoskeletal changes.[5,6]

Previous studies have primarily focused on the diagnostic performance of MRI for detecting preganglionic injuries, particularly root avulsion.[2-4] However, OBPP represents a spectrum of abnormalities that may involve multiple root levels and both preganglionic and postganglionic segments of the brachial plexus.[4,5] In addition, denervation-related muscular changes and secondary glenohumeral abnormalities may provide complementary information regarding the chronicity and severity of injury.[7,8] Despite the growing use of MRI in OBPP, studies comprehensively evaluating neural abnormalities together with associated musculoskeletal manifestations remain limited.[2]

The aim of this study was to characterize the MRI spectrum of neural injury patterns and secondary musculoskeletal changes in children with OBPP and to explore the relationship between neural abnormalities and associated musculoskeletal manifestations.

MATERIALS AND METHODS

Study Design and Patient Selection

This retrospective descriptive study was approved by the Ankara University Faculty of Medicine Human Research Ethics Committee (approval no: İ06-637-26 date: June 18, 2026) and was in accordance with the principles of the Declaration of Helsinki. The requirement for informed consent was waived due to the retrospective nature of the study. The institutional radiology database was retrospectively reviewed to identify children diagnosed with OBPP who underwent brachial plexus MRI between March 2014 and March 2026 at a tertiary referral pediatric hospital.

Inclusion criteria were a clinical diagnosis of OBPP and availability of MRI examinations with sufficient image quality for detailed assessment of neural injury patterns and secondary musculoskeletal changes. Exclusion criteria included inadequate image quality and brachial plexus injuries related to non-obstetric traumatic causes.

A total of 56 patients were included in the final study cohort.

MRI Evaluation

All MRI examinations were performed on a 1.5-T scanner (Ingenia, Philips Medical Systems, Eindhoven, The Netherlands) using a dedicated neurovascular coil. Imaging was performed with the patient in the supine position, including both shoulders, with the arms maintained in a neutral position for brachial plexus evaluation. MRI examinations were performed under institutional pediatric sedation protocols.

The MRI protocol consisted of sagittal T2-weighted turbo spin-echo (TSE), axial and coronal T1-weighted TSE (TR/TE, 600/14 ms; field of view, 16 cm; slice thickness, 2–3 mm), axial and coronal T2-weighted TSE (TR/TE, 3500/80 ms; field of view, 16 cm; slice thickness, 2–3 mm), balanced fast field echo sequences (TR/TE, 6/3 ms; field of view, 16 cm; slice thickness, 1 mm), and coronal short TI inversion recovery sequences (TR/TE, 2400/60 ms; field of view, 16 cm; slice thickness, 2–3 mm).

All MRI examinations were reviewed by a pediatric radiologist with 10 years of experience in pediatric neuroimaging. The reviewing radiologist was aware that all MRI examinations were performed for suspected OBPP, and patient age was available during image interpretation. However, the radiologist was blinded to the clinically affected side, clinical severity, physical examination findings, and other relevant clinical information.

Preganglionic abnormalities, including root avulsion and pseudomeningocele, were recorded at each root level (C5–T1). Postganglionic abnormalities were assessed at the interscalene level and included signal abnormalities, nerve thickening, and neuroma-like changes (Fig. 1). The affected root levels and involved distal brachial plexus segments (trunks, divisions, and cords) were also recorded.

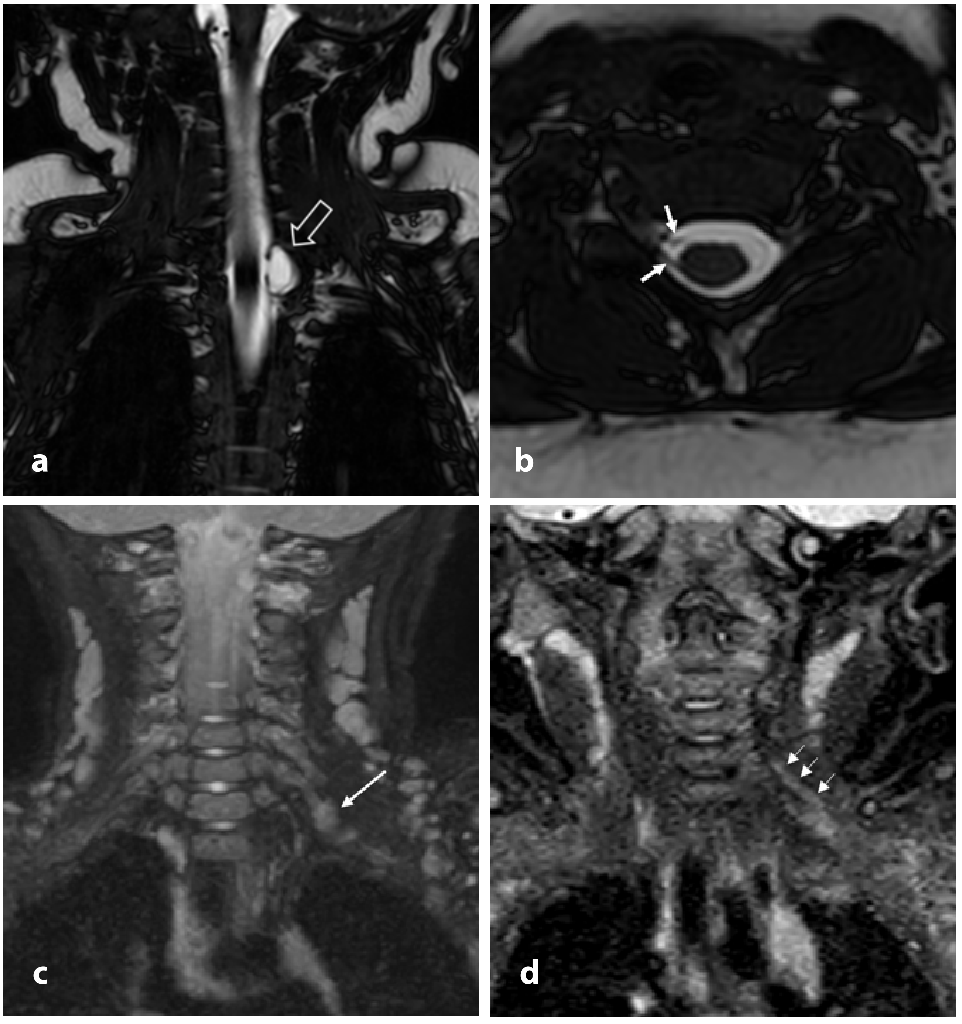

Figure 1. Representative magnetic resonance imaging findings of preganglionic and postganglionic injury in obstetric brachial plexus palsy. Coronal **(a)** and axial **(b)** heavily T2-weighted images demonstrate a left C7 pseudomeningocele (open arrow) and associated root avulsion, representing preganglionic injury. Normal dorsal and ventral nerve rootlets are shown on the contralateral side (white arrows). Coronal short TI inversion recovery (STIR) maximum intensity projection image **(c)** and coronal STIR image **(d)** demonstrate postganglionic abnormalities, including neuroma-like nodular thickening (long arrow) and asymmetric thickening with increased signal intensity of the left C5 and C6 roots at the interscalene level (short arrows).

Patients were categorized according to MRI findings as having pure preganglionic injury, pure postganglionic injury, or mixed injury (Fig. 2). Distal signal abnormalities occurring at the same level as a definite preganglionic lesion were not considered independent postganglionic injuries for classification purposes. For descriptive root-level analysis, exclusive postganglionic involvement was defined as postganglionic signal abnormality/thickening without accompanying preganglionic abnormalities at the corresponding root level.

Denervation-related muscular abnormalities were assessed in the supraspinatus, infraspinatus, subscapularis, and deltoid muscles. Muscle atrophy was graded using a semiquantitative visual scoring system: Grade 0: no atrophy, Grade 1: Mild-to-moderate atrophy, and Grade 2: Severe atrophy with marked volume loss, with or without fatty infiltration. The presence of muscle edema was recorded as a binary variable (present/absent), based on increased T2-weighted signal intensity within the affected muscle.

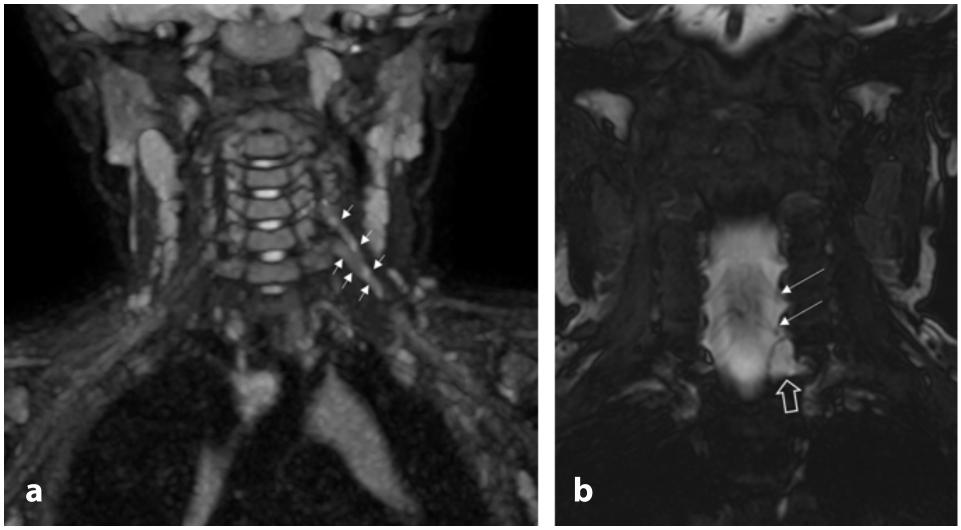

Figure 2. Mixed injury pattern in obstetric brachial plexus palsy. Coronal short TI inversion recovery maximum intensity projection image **(a)** demonstrates asymmetric thickening and increased signal intensity of the left C5 and C6 roots at the interscalene level, consistent with postganglionic injury (small arrows). In the same patient, coronal heavily T2-weighted image **(b)** demonstrates intact left C5 and C6 roots (long arrow), whereas a left C7 root avulsion and associated pseudomeningocele (open arrow) are present, consistent with preganglionic injury.

Posterior humeral head subluxation was evaluated and recorded as present or absent.

Statistical Analysis

Statistical analyses were performed using IBM Statistical Package for the Social Sciences Statistics version 23 (IBM Corp., Armonk, NY, USA). Continuous variables were expressed as median (interquartile range [IQR]), whereas categorical variables were presented as frequencies and percentages. Comparisons between categorical variables were performed using the Chi-square test or Fisher's exact test, as appropriate. Continuous variables were compared using the Mann–Whitney U-test. A two-sided $p<0.05$ was considered statistically significant.

To assess interobserver agreement, a randomly selected subset of 20 MRI examinations was independently reviewed by a second pediatric radiologist with 8 years of experience, blinded to the first reader's interpretations. Cohen's kappa was calculated for binary variables, and weighted Cohen's kappa was used for semiquantitative muscle atrophy grading.

RESULTS

A total of 56 children with OBPP were included in the study. The median age at MRI was 10.8 months (IQR, 5.4–17.0 months; range, 1.5–38.0 months). The cohort included 28 girls (50.0%) and 28 boys (50.0%); left-sided involvement was observed in 33 patients (58.9%). Demographic characteristics and overall MRI findings are summarized in Table 1.

Table 1. Demographic characteristics and overall MRI findings

Variable	Value (%)
Number of patients	56
Age at MRI, months, median (IQR; range)	10.8 (5.4–17.0; 1.5–38.0)
Female sex	28 (50.0)
Male sex	28 (50.0)
Right-sided involvement	23 (41.1)
Left-sided involvement	33 (58.9)
Pure preganglionic injury	15 (26.8)
Pure postganglionic injury	24 (42.9)
Mixed injury	17 (30.4)
Pseudomeningocele	31 (55.4)
Root avulsion	32 (57.1)
Neuroma-like thickening	16 (28.6)
Muscle edema	13 (23.2)
Any muscle atrophy	44 (78.6)
Posterior humeral head subluxation	44 (78.6)

MRI: Magnetic Resonance Imaging, IQR: Interquartile range

Eur Arch Med Res 2026;42(3):302-309

Table 2. Distribution of root-level MRI abnormalities

Root level	Overall involvement[a] *n* (%)	Pseudomeningocele *n* (%)	Root avulsion *n* (%)	Postganglionic abnormality *n* (%)	Exclusive postganglionic involvement[b] *n* (%)
C5	34 (60.7)	8 (14.3)	11 (19.6)	31 (55.4)	23 (41.1)
C6	47 (83.9)	15 (26.8)	17 (30.4)	41 (73.2)	29 (51.8)
C7	42 (75.0)	20 (35.7)	21 (37.5)	39 (69.6)	20 (35.7)
C8	20 (35.7)	6 (10.7)	6 (10.7)	17 (30.4)	13 (23.2)
T1	3 (5.4)	1 (1.8)	1 (1.8)	3 (5.4)	2 (3.6)

MRI: Magnetic resonance imaging. [a]Overall involvement was defined as the presence of any abnormality at the corresponding root level, including pseudomeningocele, root avulsion, or postganglionic signal abnormality/thickening. [b]Exclusive postganglionic involvement indicates postganglionic abnormality without a concomitant preganglionic lesion at the same root level

Based on MRI findings, pure preganglionic injury was identified in 15 patients (26.8%), pure postganglionic injury in 24 patients (42.9%), and mixed injury in 17 patients (30.4%).

Neural abnormalities involved both preganglionic and postganglionic portions of the brachial plexus. Overall root-level involvement was most frequently observed at C6 (83.9%), followed by C7 (75.0%) and C5 (60.7%). Exclusive postganglionic involvement was also most common at C6 (51.8%), followed by C5 (41.1%) and C7 (35.7%). Detailed root-level distributions of pseudomeningocele, root avulsion, postganglionic abnormalities, and exclusive postganglionic involvement are presented in Table 2.

Additional distal plexus involvement was most frequently observed at the trunk level (41.1%), followed by the division level (17.9%) and the cord level (1.8%). Neuroma-like nodular thickening was identified in 16 patients (28.6%).

Muscle atrophy was present in 44 patients (78.6%), whereas muscle edema was observed in 13 patients (23.2%). Severe atrophy (grade 2) affecting at least one muscle was identified in 4 patients (7.1%). The subscapularis and infraspinatus muscles were the most frequently affected muscles, and posterior humeral head subluxation was present in 44 patients (78.6%). No significant association was observed between injury pattern classification and the presence of muscle atrophy (Fig. 3).

The association between individual muscle atrophy and posterior humeral head subluxation is summarized in Table 3. Subscapularis muscle atrophy was significantly associated with posterior humeral head subluxation (84.1% vs. 50.0%, p=0.022), whereas infraspinatus atrophy demonstrated a similar trend that did not reach statistical significance (77.3% vs. 50.0%, p=0.081). No significant associations were observed for supraspinatus or deltoid atrophy.

Median age was significantly lower in patients with muscle edema compared to those without muscle edema (4.0 months [IQR, 2.8–6.0] versus 12.0 months [IQR, 9.1–20.0]; p<0.001).

Interobserver agreement was excellent for root avulsion (κ=1.00), pseudomeningocele (κ=0.90), neuroma-like thickening (κ=0.88), and muscle edema (κ=0.83). For semiquantitative muscle atrophy grading, weighted Cohen's kappa values were 0.78 for the supraspinatus, 0.78 for the infraspinatus, 0.83 for the subscapularis, and 1.00 for the deltoid muscle. Posterior humeral head subluxation demonstrated substantial agreement (κ=0.63). Overall, these findings indicate substantial to excellent interobserver agreement across all evaluated imaging parameters.

DISCUSSION

In this retrospective MRI-based study of children with OBPP, we comprehensively evaluated both neural injury patterns

Table 3. Association between individual muscle atrophy and posterior humeral head subluxation

Muscle atrophy	No subluxation (*n*=12)	Posterior Subluxation (*n*=44)	p
Supraspinatus atrophy, *n* (%)	4 (33.3)	16 (36.4)	1.000
Infraspinatus atrophy, *n* (%)	6 (50.0)	34 (77.3)	0.081
Subscapularis atrophy, *n* (%)	6 (50.0)	37 (84.1)	0.022*
Deltoid atrophy, *n* (%)	6 (50.0)	27 (61.4)	0.522

p-values calculated using Fisher's exact test. *p<0.05.

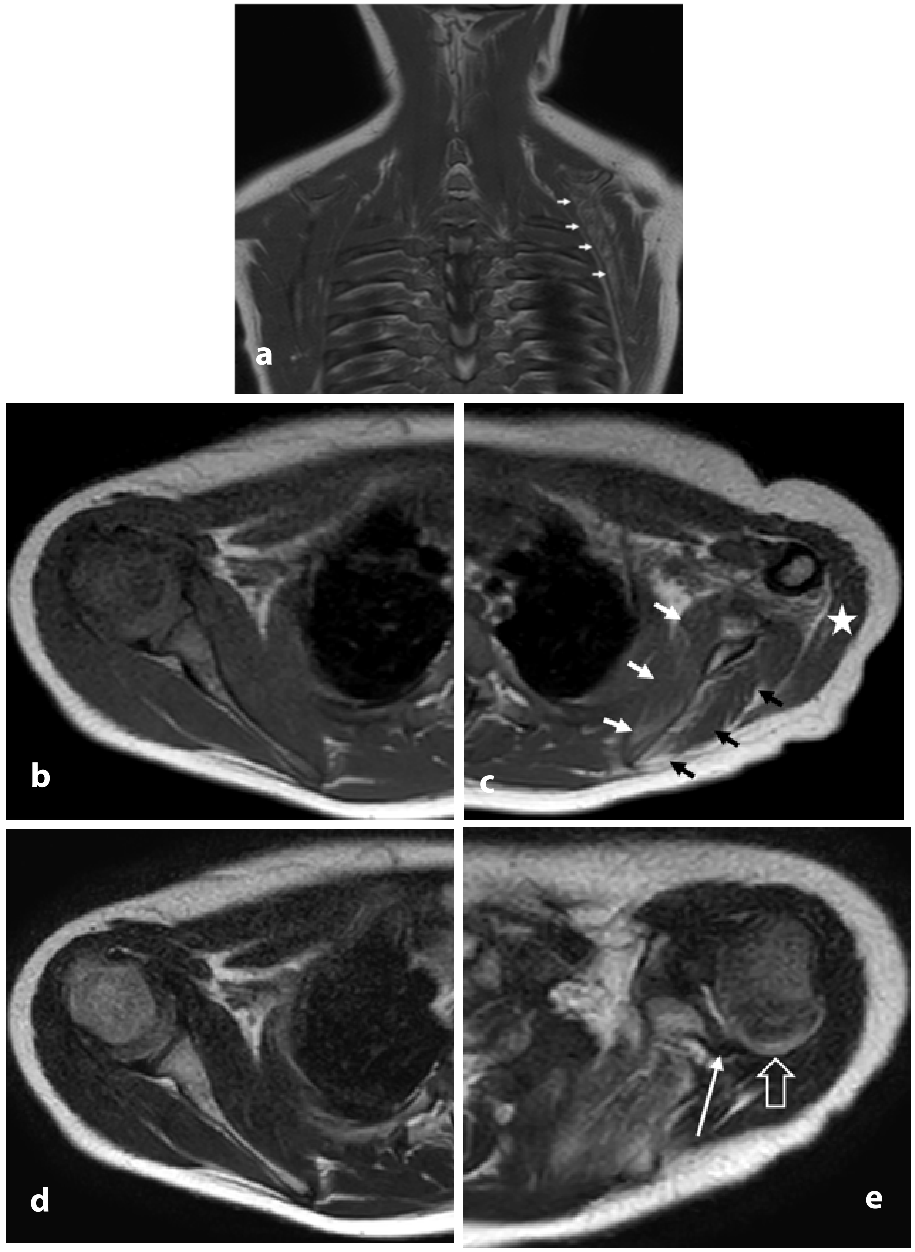

Figure 3. Secondary musculoskeletal abnormalities in obstetric brachial plexus palsy. Coronal T1-weighted image **(a)** demonstrates severe fatty atrophy of the left subscapularis muscle (short white arrows). The contralateral normal shoulder is shown in **(b)**. Axial T1-weighted image **(c)** demonstrates marked atrophy of the subscapularis (short white arrows), infraspinatus (black arrows), and deltoid muscle (asterisk). The contralateral normal shoulder is shown in **(d)**. Axial T2-weighted image **(e)**, obtained in the same patient, demonstrates posterior humeral head subluxation (open arrow) and associated glenoid dysplasia (long arrow).

and secondary musculoskeletal abnormalities. The principal findings were as follows: (1) C6 was the most frequently involved root level, followed by C7 and C5; (2) both preganglionic and postganglionic abnormalities were common, with mixed injury patterns observed in nearly one-third of patients; (3) denervation-related muscular abnormalities and posterior

Eur Arch Med Res 2026;42(3):302-309

humeral head subluxation were highly prevalent; (4) an association was observed between subscapularis muscle atrophy and posterior humeral head subluxation; and (5) muscle edema was predominantly observed in younger patients. Collectively, these findings underscore the broad spectrum of neural and musculoskeletal manifestations that can be identified on MRI in children with OBPP.

The distribution of root-level abnormalities in our cohort was generally consistent with the known predominance of upper plexus involvement in OBPP.[9-12] C6 was the most frequently involved root level, followed by C7 and C5. Although C7 abnormalities were common, isolated C7 involvement was rare, and most cases occurred in combination with C5 and/or C6 abnormalities, reflecting extended upper plexus involvement rather than isolated middle-root injury. This pattern may partly reflect referral bias, as children referred for MRI often have persistent deficits or more extensive injuries, whereas milder C5–C6 lesions may recover spontaneously and remain underrepresented in imaging-based cohorts.[2,4]

MRI demonstrated abnormalities involving both preganglionic and postganglionic portions of the brachial plexus. Pure postganglionic injury was the most common pattern; however, mixed injury was identified in approximately one-third of patients. These findings emphasize the heterogeneous nature of OBPP and highlight that preganglionic and postganglionic abnormalities frequently coexist. Although preganglionic injuries, particularly root avulsions, have traditionally received greater attention due to their prognostic significance and implications for surgical planning,[3,4,13] our findings demonstrate that postganglionic abnormalities are also common in children undergoing MRI evaluation for OBPP. Moreover, substantial rates of muscle atrophy and posterior shoulder subluxation were observed across all injury patterns. These observations suggest that clinically relevant secondary musculoskeletal changes are not limited to preganglionic injuries and may also develop in patients with postganglionic or mixed lesions. Therefore, comprehensive MRI assessment should extend beyond the detection of root avulsion and include evaluation of distal neural abnormalities and their musculoskeletal consequences.

Secondary musculoskeletal abnormalities were highly prevalent in our cohort. Overall, muscle atrophy and posterior shoulder subluxation were each observed in 78.6% of patients. Among the evaluated muscles, subscapularis and infraspinatus were the most frequently affected. The predominance of subscapularis and infraspinatus involvement is consistent with previous reports describing substantial denervation-related changes in the shoulder girdle muscles of children with OBPP.[7,8,14] The higher frequency of posterior shoulder subluxation among patients with subscapularis atrophy in our cohort is consistent with the proposed role of denervation-related muscle imbalance in the development of glenohumeral deformity in OBPP.[7,8] However, because this was an exploratory analysis involving multiple comparisons, this finding should be interpreted with caution. Previous studies have shown that glenohumeral instability and posterior humeral head subluxation may develop during early infancy and progressively evolve into secondary glenohumeral deformity, underscoring the importance of recognizing shoulder involvement in children with persistent OBPP.[15,16]

The frequency of muscle atrophy did not differ significantly across injury patterns, whereas muscle edema was significantly more common in younger patients. Together, these findings suggest that denervation-related muscle changes may not be determined solely by the anatomical pattern of neural injury. Factors such as injury severity, duration of denervation, and timing of imaging may also contribute to the extent of muscular involvement observed on MRI. Given the recognized progression from denervation edema to chronic muscle atrophy, the pattern of muscular abnormalities may vary according to the stage of denervation at the time of imaging.[17,18]

Limitations

The present study has several limitations. First, its retrospective design may have introduced selection bias. Second, surgical findings, electrodiagnostic studies, and long-term clinical outcomes were not consistently available for correlation with MRI findings. Therefore, the diagnostic accuracy of individual MRI findings could not be systematically assessed. Third, muscle atrophy was evaluated using a semiquantitative visual grading system rather than quantitative volumetric measurements. The analyses evaluating the association between individual muscle atrophy and posterior humeral head subluxation were exploratory. As multiple comparisons were performed without formal adjustment, these findings should be interpreted with caution and require confirmation in larger studies. Finally, this was a single-center study, which may limit the generalizability of our findings. Although the study covered a 12-year period, all MRI examinations were performed on the same MRI scanner using a standardized institutional imaging protocol, reducing potential variability in image acquisition. Nevertheless, this study provides a comprehensive overview of both neural and musculoskeletal MRI findings in children with OBPP.

CONCLUSION

MRI demonstrates a broad spectrum of neural and musculoskeletal abnormalities in children with OBPP. In addition to characterizing preganglionic and postganglionic injury patterns, MRI provides valuable information regarding secondary musculoskeletal changes, including muscle denervation and glenohumeral deformity. These findings highlight the value of MRI in the comprehensive evaluation of OBPP, extending beyond the detection of root avulsion to include associated distal neural and musculoskeletal abnormalities.

Disclosures

Ethics Committee Approval: The study protocol was approved by the Ankara University Faculty of Medicine Human Research Ethics Committee (No: İ06-637-26, Date: 18/06/2026).

Informed Consent: The requirement for informed consent was waived due to the retrospective nature of the study.

Conflict of Interest: The authors declare that there is no conflict of interest.

Funding: The authors received no financial support for the research and/or authorship of this article.

Use of AI for Writing Assistance: During the preparation of this manuscript, the authors used Paperpal (Cactus Communications, Princeton, NJ, USA) for English language editing and text refinement. The authors reviewed and edited the manuscript as necessary and take full responsibility for the content of the manuscript.

Authorship Contributions: Concept – SKS; Design – SKS, SF; Supervision – SF; Fundings – SKS, EA, BU; Materials – SKS, EA, BU; Data collection &/or processing – SKS, EA, BU; Analysis and/or interpretation – SKS, SF; Literature search – SKS; Writing – SKS; Critical review – SKS, EA, BU, SF.

Peer-review: Externally peer-reviewed.

REFERENCES

1. Hardie CM, Karia C, Wade RG, Kraft JK, Bains R, Bourke G. Magnetic resonance imaging for detecting root avulsions in brachial plexus birth injuries. J Hand Surg Eur Vol 2026;51:589–96.
2. Girard AO, Suresh V, Lopez CD, Seal SM, Tuffaha SH, Redett RJ, et al. Radiographic imaging modalities for perinatal brachial plexus palsy: a systematic review. Childs Nerv Syst 2022;38:1241–58.
3. Brooks J, Hardie C, Wade R, Teh I, Bourke G. Diagnostic accuracy of MRI for detecting nerve injury in brachial plexus birth injury. Br J Radiol 2025;98:36–44.
4. Somashekar DK, Wilson TJ, DiPietro MA, Joseph JR, Ibrahim M, Yang LJ, et al. The current role of diagnostic imaging in the preoperative workup for refractory neonatal brachial plexus palsy. Childs Nerv Syst 2016;32:1393–7.
5. Shen PY, Nidecker AE, Neufeld EA, Lee PS, James MA, Bauer AS. Non-sedated rapid volumetric proton density MRI predicts neonatal brachial plexus birth palsy functional outcome. J Neuroimaging 2017;27:248–54.
6. Gunes A, Bulut E, Uzumcugil A, Oguz KK. Brachial plexus ultrasound and MRI in children with brachial plexus birth injury. AJNR Am J Neuroradiol 2018;39:1745–50.
7. Pöyhiä TH, Nietosvaara YA, Remes VM, Kirjavainen MO, Peltonen JI, Lamminen AE. MRI of rotator cuff muscle atrophy in relation to glenohumeral joint incongruence in brachial plexus birth injury. Pediatr Radiol 2005;35:402–9.
8. Balloufaud M, Hosni S, Bolivar J, Saguintaah M, Virassamy M, Laffont I, et al. Subscapularis impairment on magnetic resonance imaging is correlated with functional limitations in neonatal brachial plexus palsy. Int Orthop 2024;48:1635–43.
9. Somashekar D, Yang LJ, Ibrahim M, Parmar HA. High-resolution MRI evaluation of neonatal brachial plexus palsy: A promising alternative to traditional CT myelography. AJNR Am J Neuroradiol 2014;35:1209–13.
10. Doumouchtsis SK, Arulkumaran S. Are all brachial plexus injuries caused by shoulder dystocia? Obstet Gynecol Surv 2009;64:615–23.
11. Malessy MJ, Pondaag W. Nerve surgery for neonatal brachial plexus palsy. J Pediatr Rehabil Med 2011;4:141–8.
12. Menashe SJ, Tse R, Nixon JN, Ishak GE, Thapa MM, McBroom JA, et al. Brachial plexus birth palsy: multimodality imaging of spine and shoulder abnormalities in children. AJR Am J Roentgenol 2015;204:W199–206.
13. Szaro P, Geijer M, Ciszek B, McGrath A. Magnetic resonance imaging of the brachial plexus. Part 2: Traumatic injuries. Eur J Radiol Open 2022;9:100397.
14. van Gelein Vitringa VM, van Kooten EO, Mullender MG, van Doorn-Loogman MH, van der Sluijs JA. An MRI study on the relations between muscle atrophy, shoulder function and glenohumeral deformity in shoulders of children with obstetric brachial plexus injury. J Brachial Plex Peripher Nerve Inj 2009;4:5. Erratum in: J Brachial Plex Peripher Nerve Inj 2009;4:9.
15. Waters PM, Smith GR, Jaramillo D. Glenohumeral deformity secondary to brachial plexus birth palsy. J Bone Joint Surg Am 1998;80:668–77.
16. van der Sluijs JA, van Ouwerkerk WJ, de Gast A, Wuisman P, Nollet F, Manoliu RA. Retroversion of the humeral head in children with an obstetric brachial plexus lesion. J Bone Joint Surg Br 2002;84:583–7.
17. Deshmukh SD, Samet J, Fayad LM, Ahlawat S. Magnetic resonance neurography of traumatic pediatric peripheral nerve injury: beyond birth-related brachial palsy. Pediatr Radiol 2019;49:954–64.
18. Kamath S, Venkatanarasimha N, Walsh MA, Hughes PM. MRI appearance of muscle denervation. Skeletal Radiol 2008;37:397–404.